Destruction of Conductance Fluctuations in a Dirty Wire

Ningjia Zhu, Hong Guo, and R. Harris
Center for the Physics of Materials and Department of Physics, McGill University, Rutherford Physics Building, Montréal, Québec, Canada H3A 2T8
(Received 25 April 1996)

We study the conductance fluctuations of a dirty quantum wire in which both mesoscopic and ballistic transport features play a role. The existence of a ballistic transport channel destroys the universal conductance fluctuations, so that the "mixed" transport regime is marked by nonuniversal fluctuations which we compute both analytically, using a diagrammatic technique, and with a numerical evaluation of the Landauer formula. The crossover behavior of the fluctuation amplitude from the usual quasi-1D situation to that of the mixed regime is clearly revealed, and the role of various length scales are identified. [S0031-9007(96)01038-1]

PACS numbers: 73.20.Dx, 72.10.–d, 73.50.Bk

Over the last decade an extensive research effort has been devoted to the understanding of the quantum transport properties of various submicron scale electronic structures [1]. A main motivation of this effort has been to develop potentially useful electronic devices whose operation is based on quantum phenomena. There are three important length scales associated with a quantum conductor: the system linear size L, the elastic mean free path l, and the electron phase coherence length ξ. Here l is essentially determined by the impurity concentration, and ξ is fixed by various phase breaking events. When L is much larger than the other two scales we have the usual classical Drude conduction. On the other hand, if $l < L < \xi$, the diffusive motion of the conduction electrons maintains their phase coherence, leading to the so called mesoscopic regime of quantum transport, where the most interesting phenomenon is the universal conductance fluctuations (UCF) [2]. The mesoscopic transport regime is the subject of extensive studies. Finally, when the system size is even smaller, $L < l < \xi$, we enter the ballistic regime where electrons traverse the conductor ballistically without, on average, suffering impurity scattering. In this situation, the factor which limits the current is the scattering at the boundaries of the conductor, and the conductance can be computed by the Landauer theory of one-dimensional transport. The ballistic regime has also been studied in detail both experimentally and theoretically [1].

Many situations of potential interest for device applications have both mesoscopic and ballistic ingredients. For instance, it is known that the electron mobility in a metal-oxide-semiconductor field-effect transistor is substantially influenced by the quality of the Si-SiO_2 interface, and parameters characterizing scattering at the rough interface can be extracted from experimental data [3]. Similarly, for a quantum MESFET [4] the roughness at the metal-semiconductor interface provides the "impurity scattering." Equally, as freestanding quantum wires become a reality, one must deal with the impurity scattering problem near the boundaries, as impurities tend to diffuse into the wire in this region. It is also known that scattering at irregular interfaces of a short-period superlattice and impurity scattering in a double-barrier quantum well have an important influence on quantum tunneling I-V characteristics [5].

In all these situations the devices possess regions where impurity scattering is important, and regions where very little impurity scattering is present. From a theoretical point of view these are difficult problems because one has to deal with a spatially nonuniform system. Furthermore, many conceptual difficulties arise concerning this "mixed" regime of quantum transport, such as the destruction of UCF by the ballistic channels, the competition of localization effects and ballistic effects, the contributions of transverse subbands which are smeared by the impurity scattering, and more importantly the role played by various length scales. So far, theoretical studies of this mixed transport regime have focused on the important problem of a narrow quantum wire [6] with rough boundaries [7–9], and investigations of conductance fluctuations in these systems have been limited to numerical calculations. While useful intuition has been obtained, it is nevertheless difficult to draw general conclusions from purely numerical investigations since accurate values of the conductance fluctuations as a function of system parameters are difficult to obtain.

It is the purpose of this work to provide both diagrammatic and numerical analyses of this mixed regime, with a focus on the important conceptual questions mentioned above. In particular, we consider a two-dimensional "dirty" quantum wire with length L and width W, as shown in the inset of Fig. 1. Along the two walls of the wire, a layer of thickness t is distributed randomly with impurities of scattering potential [2] $V_i = u\delta(\mathbf{r} - \mathbf{r}_i)$, where u is the strength of the scattering, $\mathbf{r}_i$ is the location of the ith impurity, and $\mathbf{r}$ is the electron coordinates. The Hamiltonian has the form

$$\mathcal{H} = \sum_{\mathbf{p}} \epsilon_{\mathbf{p}} a^{\dagger}_{\mathbf{p}} a_{\mathbf{p}} + \sum_{\mathbf{q}} u[\rho^{u}_{\mathbf{q}} + \rho^{l}_{\mathbf{q}}] \cdot \sum_{\mathbf{p}} a^{\dagger}_{\mathbf{p}+\mathbf{q}} a_{\mathbf{p}} , \quad (1)$$

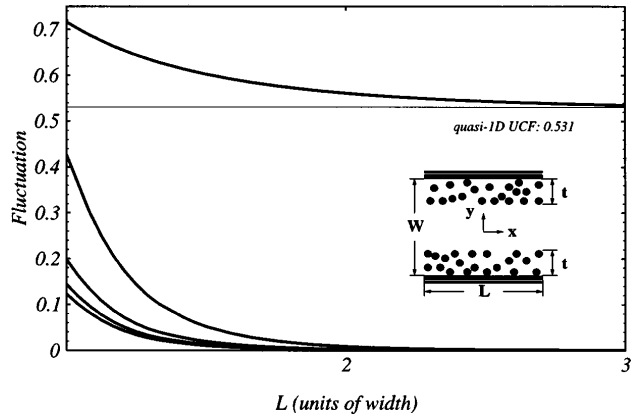

FIG. 1. Conductance fluctuation $[\mathrm{rms}(g)]^2$ [units in $(e^2/h)^2$] as a function of wire length L (units in W), for the approximate theory neglecting the $p_\perp$ dependence in the self-energy. Curves from top down correspond to $t = W/2, W/3, W/4, W/5$, and $W/6$. Inset is a schematic drawing of the dirty wire.

where $a^\dagger_{\mathbf{p}}$ and $a_{\mathbf{p}}$ are creation and annihilation operators for momentum $\mathbf{p}$, $\epsilon_{\mathbf{p}}$ is kinetic energy of electrons with effective mass m^*, and $\rho^u_{\mathbf{q}} = \sum_i^{\text{upper}} e^{-i\mathbf{q}\cdot\mathbf{r}_i}$ and $\rho^l_{\mathbf{q}} = \sum_i^{\text{lower}} e^{-i\mathbf{q}\cdot\mathbf{r}_i}$ are the impurity densities in the upper and lower impurity layers.

Clearly, if $W = 2t$ we recover a quasi-1D mesoscopic conductor whose transport properties are well understood. On the other hand, when $W > 2t$ the system may possess both mesoscopic *and* ballistic behavior. To our knowledge there are as yet no analytical studies of transport in this important general regime, or of the free-standing dirty quantum wire in particular. Furthermore, whereas the impurity scattering is somewhat different from rough wall scattering, the physics should be similar and our work thus provides additional theoretical understanding of the numerical results reported so far on roughness scattering [7–9].

The diagrammatic analysis proceeds along similar lines to that for a mesoscopic conductor with *uniformly* distributed impurities [2]. However, since in our case the impurity distribution is nonuniform, the algebra becomes extremely tedious [10]. In particular one has to pay special attention to the transverse direction (the y direction) in all calculations. The nonuniformity leads to important differences, as compared to the usual quasi-1D mesoscopic conductor, in various quantities such as the self-energy of the one-particle Green's function, the vertices and the diffusion operator, and indeed in the general behavior of the predicted conductance fluctuations. To save space in the following we outline only the most important modifications and present the details elsewhere [10].

Retaining up to the second order perturbation terms we obtain the imaginary part of the self-energy in the one-particle Green's function as a function of the transverse momentum $p_\perp$ in the following form:

$$\Gamma(p_\perp) = \frac{2u^2 N_i m^* WL}{\hbar^3} \times \left[1 + \frac{1}{2|p_\perp|L}\{N_i[1 + |f_{p_\perp}(t)|^2] + 1 + f^r_{p_\perp}(t)\}\right], \quad (2)$$

where N_i is number of impurities in each impurity layer (assumed to be the same in both layers). The function $f_{p\perp}$ gives the impurity distribution away from the wall which is assumed to be Gaussian: $f_{p_\perp}(t) = \int_0^t e^{-\gamma z^2} e^{2ip_\perp z}\, dz / \int_0^t e^{-\gamma z^2}\, dz$. $f^r_{p_\perp}(t)$ is the real part of $f_{p_\perp}(t)$. The parameter γ controls the width of the distribution: a very small γ gives essentially a uniform distribution in the layer t, while a larger γ gives a diffusive distribution with higher concentration of impurities near the quantum wire boundary. To compute the conductance fluctuations via a diagrammatic technique, we follow the self-consistent conductance fluctuation theory [2] by considering the Feymann diagrams with all possible double, triple, and quadruple bubble-bubble connections [10].

Before presenting the complete result, we can get a first hint of the effects of our nonuniform impurity distribution by simply neglecting the $p_\perp$ dependence of the self-energy. This gross approximation makes the algebra very similar to the usual UCF calculations, and the diffusion propagator becomes isotropic: $\sim 1/q^2$. In Fig. 1 we plot the conductance fluctuations $[\mathrm{rms}(g)]^2$ as a function of the wire length L for various impurity layer thickness t. To obtain the numerical values we have fixed the system parameters as electron energy $kW = 55$ with k the Fermi wave vector, $W = 3250$ Å, $u = 0.01$ meV, $N_i = 40$, and effective mass $m = 0.067m_e$ with m_e the bare mass of the electron. It is clearly seen that for $t = W/2$, i.e., without a ballistic region, the conductance fluctuations $[\mathrm{rms}(g)]^2$ approach the quasi-1D universal value $0.531(e^2/h)^2$ as L is increased. However, when there is a ballistic region in the dirty wire, i.e., for $t = W/3$, $W/4$, $W/5$, and $W/6$ (see Fig. 1), the conductance fluctuations vanish smoothly when the length of the wire is increased. This is understandable from the point of localization [7]. For our wire, the ballistic channel in the center is always conducting for electron energies above the propagation threshold, and therefore essentially does not contribute to the fluctuations. Indeed, the fluctuations are mostly contributed by the impurity layers, and they diminish when the system length L is close or beyond the localization length of the layers. It is well known that a very thin layer of impurities will have a smaller localization length than that of a thicker layer for a given impurity density [7], since the small lateral size limits the conduction channel. Thus for smaller values of t we expect a smaller localization length, and the fluctuations should fall faster as L is increased, a physical picture which is consistent with Fig. 1. We note that the general behavior discussed here is quite similar to that found in various numerical simulations on the rough

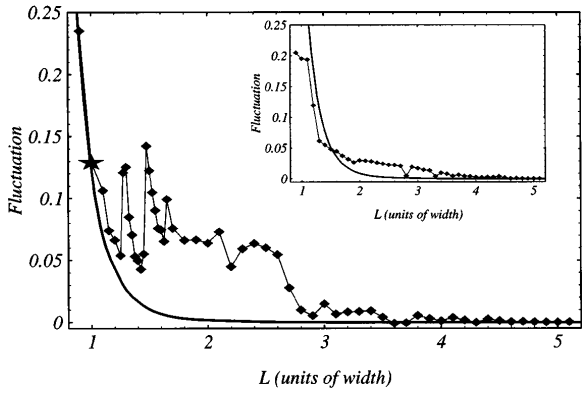

FIG. 2. The solid squares give $[\mathrm{rms}(g)]^2$ as a function of L for $t = W/6$ from the full theory including all the $p_\perp$ dependence. The smooth solid curve is the result from the approximate theory. The star point is the result from the finite-element numerical simulation. Inset: the results for $t = W/3$.

wall scattering [7–9]. In addition, for systems where two separate disordered reservoirs are connected by a pure ballistic region, the conductance fluctuations can also be suppressed under certain conditions as shown in Ref. [11].

When we include the explicit $p_\perp$ dependence in the analysis, a major difference is the change of the diffusion [12] operator, which becomes [10]

$$1 - u^2 N_i \left[\frac{3}{4}\,\Pi^{(1)} + i\Pi^{(2)}\Delta E \right] - \frac{1}{2}\,u^2 N_i v_F^2 \Pi^{(3)} \frac{\partial^2}{\partial x^2} + i u^2 N_i v_F \Pi^{(4)} \frac{\partial^2}{\partial x \partial y} - u^2 N_i \left[\frac{1}{2}\,v_F^2 \Pi^{(3)} - i v_F \Pi^{(4)} + \frac{1}{4}\,\Pi^{(5)} \right] \frac{\partial^2}{\partial y^2}, \quad (3)$$

where $\Pi^{(1)} = \hbar^{-1} \int dp_\perp N_{\epsilon-\epsilon_\perp} \tau(p_\perp)$, $\Pi^{(2)} = \hbar^{-2} \times \int dp_\perp N_{\epsilon-\epsilon_\perp} \tau^2(p_\perp)$, $\Pi^{(3)} = \hbar^{-1} \int dp_\perp N_{\epsilon-\epsilon_\perp} \tau^3(p_\perp)$, $\Pi^{(4)} = \hbar^{-1} \int dp_\perp N_{\epsilon-\epsilon_\perp} \tau(p_\perp)\alpha(p_\perp)$, $\Pi^{(5)} = \hbar^{-1} \times \int dp_\perp N_{\epsilon-\epsilon_\perp} [\alpha(p_\perp)]^2/\tau(p_\perp)$, $\tau(p_\perp) = \hbar/\Gamma(p_\perp)$, $\alpha(p_\perp) = \frac{\partial \tau(p_\perp)}{\partial p_\perp}$. v_F is the Fermi velocity, and $N_{\epsilon-\epsilon_\perp}$ is the 1D density of states. ΔE is the correlation energy,

$$\Delta E = t v_F^2 \overline{\tau(p_\perp)} \hbar / L^2 W + (1 - 2t/W) \hbar v_F / \sqrt{LW},$$

which is a combination of both a ballistic part and a diffusive part, with $\overline{\tau(p_\perp)}$ an average value of $\tau(p_\perp)$ over momentum $p_\perp$. Although the diffusion operator is now much more complicated, it is fortunate that its eigenfunctions can still be obtained in closed form, and are found to be the zeroth order Bessel functions of complex argument [10]. By contrast, the eigenfunctions for the isotropic case are the simple box-normalized sinusoidal functions. Given the eigenfunctions, we follow the usual procedure [2] to compute the conductance fluctuations.

The general behavior of the conductance fluctuation as a function of the wire length L is similar to the approximate result presented in Fig. 1. In Fig. 2 and its inset, we plot the results (the data points) for impurity layer thickness $t = W/6$ and $t = W/3$. For comparison, the smooth curves show the approximate result where the anisotropy (i.e., $p_\perp$ dependence) is neglected. Several observations are in order. First, the conductance fluctuation $[\mathrm{rms}(g)]^2$ drops rapidly as L increases and becomes very small for large values of L. This behavior is consistent with all previous numerical simulations of boundary roughness scattering where it was attributed to the role of localization effect [7–9]. For example, the numerical simulation data of a wire with rough boundaries [9] shows that the conductance fluctuations decrease approximately exponentially with L. Second, there are clear oscillations of $[\mathrm{rms}(g)]^2$ as L is increased (see the data points in Fig. 2). These are not present in the "isotropic theory," which is understandable since it does not respect the lateral anisotropy and quantization. We have checked that when $[\mathrm{rms}(g)]^2$ is plotted against other parameters such as the electron Fermi energy or the impurity layer thickness t, similar oscillations are also observed. This indicates that the oscillations result from resonance behavior since wave functions and their derivatives must match across the different layers in the wire. It is interesting to note that when the impurity layer thickness is large, e.g., $t = W/3$, the full theory and the grossly simplified isotropic theory give quantitatively similar results, as shown in the inset of Fig. 2. Obviously the dirty wire with a larger t is closer to that of a quasi-1D mesoscopic conductor and hence more "isotropic" as far as the impurity scattering self-energy is concerned. Finally, the data for $t = W/6$ has a rapid drop at $L \sim 3W$ (Fig. 2). This behavior is likely to be related to the localization effect discussed above: the fluctuations diminish when L approaches the localization length of the impurity layers. Indeed, for a rough-boundary wire the numerically fitted localization length [9] was $\sim 5W$ for a roughness amplitude of $\sim W/10$. If our impurity layer thickness t plays the role corresponding to the roughness amplitude, our result is of the same order of magnitude as in the numerical simulations.

An alternative study of the same problem is provided by direct numerical simulations employing the Landauer formula to compute the conductance in terms of transmission coefficients. This not only provides a quantitative check of our analytical results, but also shows how the contributions of successive propagating subbands contribute to the conductance fluctuations. The quantum scattering in the same dirty quantum wire system is solved using the single electron effective mass Schrödinger equation by a finite element numerical scheme detailed in Ref. [13]. This method allows us to obtain quantitatively accurate results. For incoming electron energy $kW = 55$ there are 17 subbands to be computed individually and their contributions are shown in Fig. 3. Typically we have used 550 to 1000 (the largest 5000) independent impurity configurations for impurity averaging of each subband [14].

Using this numerical simulation technique, we first verified that with $kW = 55$ and $t = W/2$, i.e., for a quasi-1D mesoscopic wire, we were indeed in the usual UCF

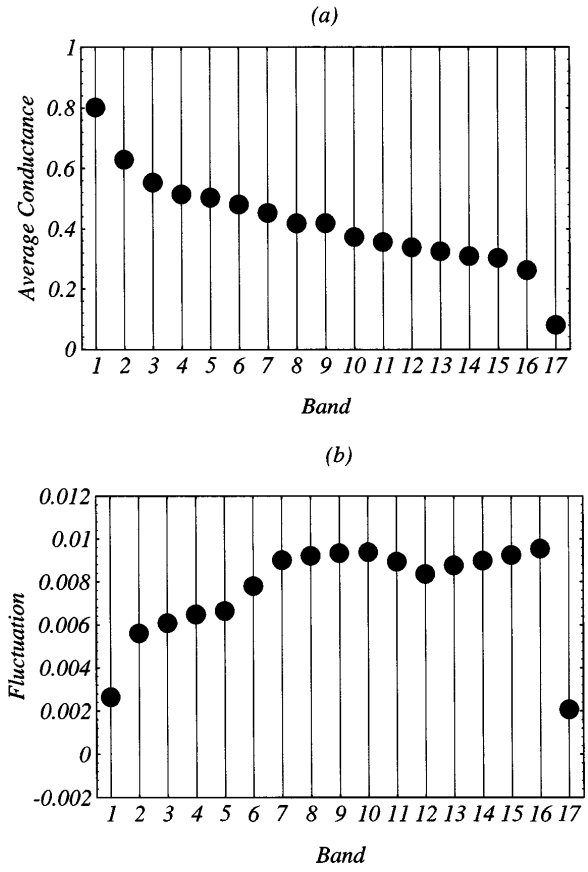

FIG. 3. Results from the finite-element numerical simulation. (a) The average conductance for each of the 17 subbands. (b) The fluctuations $[\mathrm{rms}(g)]^2$ for all the subbands. The system parameters are $t = W/6$, $L = W = 3250$ Å, $N_i = 40$, $kW = 55$.

regime. We also found that at around $kW = 55$ the conductance fluctuations are almost independent of the Fermi energy: this is why we have fixed the energy at this value [7]. From Fig. 3, it is clear that for $t = W/6$ ($L = W$) the impurity-averaged conductance of each successively higher subband is progressively smaller. This is because the higher the subband, the smaller its longitudinal (x direction) momentum, and with smaller longitudinal momentum it is more difficult for an electron to traverse the dirty wire. This is also consistent with the numerical simulations of rough boundary scattering [7]. On the other hand, the conductance fluctuations [Fig. 3(b)] for the lowest and highest subbands are smaller than those of the middle subbands. This peculiar behavior is due to the upper and lower bounds of the conductance which each transport subband can contribute: e^2/h or zero. Since the lowest and highest subbands contribute values close to these bounds [see Fig. 3(a)], their fluctuations are limited by them. When adding up all the contributions according to the Landauer formula, we obtain the conductance fluctuations for this set of parameters as $(0.13 \pm 0.01)\,(e^2/h)^2$, in almost perfect agreement with our analytical prediction of $0.129(e^2/h)^2$. The numerical data point is shown as a star in Fig. 2.

In summary, we have investigated for the first time the conductance fluctuations of a dirty quantum wire with impurities concentrated near the wire boundaries, using both a diagrammatic technique and a numerical method. The crossover from an anisotropic diffusive propagator to that of an isotropic one is clearly revealed. Because of the presence of a ballistic region, the conductance fluctuations are not universal and depend on system parameters such as the impurity layer thickness t. The fluctuations decay with the wire length L for a given t, and such a decay is faster for wires with smaller t. This is due to electron localization in the impurity layers. The general behavior predicted by our analytical approach is consistent with previous numerical simulations on roughness scattering, and is quantitatively confirmed by our numerical simulations of the model.

We gratefully acknowledge support by the Natural Sciences and Engineering Research Council of Canada and le Fonds pour la Formation de Chercheurs et l'Aide à la Recherche de la Province du Québec.

[1] H. van Houten and C. W. J. Beenakker, in *Solid State Physics*, edited by H. Ehrenreich and D. Turnbull (Academic, San Diego, 1991), Vol. 44.
[2] P. A. Lee, A. D. Stone, and H. Fukuyama, Phys. Rev. B **35**, 1039 (1987); For a recent review, see, for example, J. Rammer, Rev. Mod. Phys. **63**, 781 (1991).
[3] T. J. Krutsick, M. H. White, Hon-Sum Wong, and R. V. Booth, IEEE Trans. Electron Devices **34**, 1676 (1987).
[4] M. C. Yalabik, G. Neofotistos, K. Diff, Hong Guo, and J. D. Gunton, IEEE Trans. Electron Devices **36**, 1009 (1989).
[5] A. R. Bonnefoi, D. H. Chow, and T. C. McGill, J. Appl. Phys. **62**, 3836 (1987); S. K. Kirby, D. Z.-Y Ting, and T. C. McGill, Phys. Rev. B **48**, 15 237 (1993).
[6] T. J. Thornton, M. L. Roukes, A. Scherer, and B. P. Van de Gaag, Phys. Rev. Lett. **63**, 2128 (1989).
[7] T. Ando and H. Tamura, Phys. Rev. B **46**, 2332 (1992); H. Tamura and T. Ando, *ibid.* **44**, 1792 (1991); H. Akera and T. Ando, *ibid.* **43**, 11 676 (1991).
[8] K. Nikolić and A. Mackinnon, Phys. Rev. B **50**, 11 008 (1994).
[9] R. Harris and Hong Guo, Phys. Rev. B **51**, 5491 (1995).
[10] The detailed algebra will be presented elsewhere.
[11] D. L. Maslov, C. Barnes, and G. Kirczenow, Phys. Rev. Lett. **70**, 1984 (1993); Phys. Rev. B **48**, 2543 (1993).
[12] G. Bergman, Phys. Rep. **107**, 1 (1984).
[13] C. S. Lent, Appl. Phys. Lett. **67**, 6353 (1990).
[14] The extremely large CPU time requirement for the numerical simulations prevented us from obtaining more points for comparison. For one set of system parameters (t, L) and averaging over 1000 impurity configurations for each of the 17 propagating subbands, the total computation took about 1100 CPU hours on a SGI R8000 processor.